Biochemistry

 Volume 19, Number 16 August 5, 1980

# Properties of Human Apolipoprotein A-I at the Air–Water Interface†

Betty W. Shen* and Angelo M. Scanu

ABSTRACT: In order to study the properties and structure of human apolipoprotein A-I (apo-A-I) at the air-water interface, we formed monolayers of apo-A-I by either spreading or spontaneous adsorption from the subphase. The rate of monolayer formation, force–area (II–A) curves, and surface potentials were analyzed quantitatively. We constructed force–area curves by keeping constant either (a) the total area or (b) the total number of molecules. The results obtained by method a were reproducible and superimposable with those obtained from adsorbed monolayers. In turn, the results obtained by method b indicated aging effects by both pressure and potential measurements, suggesting irreversible denaturation of apo-A-I at areas larger than 50 Å$^2$/amino acid. At pressures lower than 0.5 dyn/cm, apo-A-I monolayers followed the two-dimensional ideal gas law; the molecular weight of the apoprotein calculated from the intercept on the ordinate of the $\Pi A$ vs. $\Pi$ plot had an average value of 25 000. At higher pressures, the monolayer deviated from ideality, and the surface pressure increased curvilinearly as the area decreased. A semiempirical equation derived for the surface isotherm of the apo-A-I monolayer fitted both our experimental data and those for protein monolayers reported in literature. Kinetic studies on the adsorption and dissolution of apo-A-I with and without stirring of the subphase indicated that the formation of the apo-A-I monolayer is a reversible, diffusion-controlled process and that there is a fast equilibrium between the molecules at the interface and in solution. Taken together, the results demonstrate that apo-A-I is a surface-active molecule with unique properties. The flexibility of apo-A-I at the air–water interface indicates that the conformational change at this interface requires only a small change in free energy, a finding which parallels the reported behavior of apo-A-I in solution. The rapid equilibration between apo-A-I molecules at the surface and those in the bulk phase may account for the exchange of this apolipoprotein among lipoproteins.

Recent physical and chemical studies on both high-density lipoproteins (HDL) and low-density lipoproteins (LDL) have suggested that apoproteins, cholesterol, and phospholipids form a monolayer at the outer surface of these lipoproteins (Morrisett et al., 1975). The enzymatic proteolysis of the intact lipoproteins (Aggerbeck et al., 1976; Camejo, 1969; Pattnaik et al., 1976) results in aggregation, indicating that the apoproteins play an important role in maintaining the lipoprotein structure. Such stabilization should be intimately related to the surface properties of the apoproteins. In order to explore the behavior of apolipoproteins at amphiphilic interfaces and their relation to the surface organization of human serum $HDL_3$, we turned our attention to apolipoprotein A-I (apo-A-I), which is the major protein component of plasma HDL. Apo-A-I was chosen for this investigation because (1) it is the only major protein that is always present in naturally occurring HDL, (2) it can be obtained in reasonably large quantities in a pure state, (3) its solution properties are reasonably well understood (Baker et al., 1974; Formisano et al., 1978; Osborne & Brewer, 1977; Vitello & Scanu, 1976), and (4) under appropriate conditions, it can combine with lipids to form a particle that is indistinguishable from native HDL (Ritter & Scanu, 1977).

Previous studies (Camejo et al., 1968, 1970; Davis et al., 1973; Phillips et al., 1975a,b) have shown that the mixture of apoproteins of HDL (apo-HDL) from rats, man, and pigs tends to accumulate and to form mixed monolayers with phospholipids at the air–water interface more readily than other globular proteins. Stimulated by these observations, we have undertaken the quantitative analysis of the surface properties of pure apolipoproteins. The air–water interface was chosen as the simplest experimental model of the amphiphilic lipoprotein surface, since numerous well-established experimental methods are available by which the surface properties of macromolecules can be assessed.

In the present investigation, we studied the surface behavior of monolayers of pure human apo-A-I by combining measurements of surface pressure and surface potential. The time and pressure dependence of monolayer formation, the surface isotherms, and the kinetics of adsorption and desorption of the

† From the Departments of Medicine and Biochemistry, The University of Chicago, and The Franklin McLean Memorial Research Institute (operated by the University of Chicago for the U.S. Department of Energy under Contract EY-76-C-02-0069), Chicago, Illinois 60637. *Received January 22, 1980.* This work was supported by Grants 1 P17 HL 15062 and 1 P01 HL 18577 from the National Heart and Lung Institute and by Grants 79-131 and 78-1070 from the American and Chicago Heart Association.

* Correspondence should be addressed to this author at The University of Chicago, Department of Medicine, Chicago, IL 60637. She is an Established Investigator of the American Heart Association.

0006-2960/80/0419-3643$01.00/0 

protein monolayers were analyzed quantitatively. The results show that apo-A-I has a high surface activity at the air–water interface which can contribute to our understanding of the behavior of this apoprotein at the HDL surface. A preliminary account of some of these experiments has been published (Shen et al., 1973; Shen & Scanu, 1979).

## Experimental Section

### *Materials*

Apo-A-I was isolated from delipidated HDL by Sephadex G-200 column chromatography in 8 M urea, followed by DEAE ion-exchange chromatography in 6 M urea (Scanu et al., 1969). The final product gave a single band by sodium dodecyl sulfate–polyacrylamide gel electrophoresis and had the amino acid composition reported earlier (Scanu et al., 1972). The protein was lyophilized and stored at −20 °C. For every set of experiments, fresh stock solutions of apo-A-I were prepared in 0.01 M phosphate buffers at the appropriate pH. Radioactively labeled apo-A-I ([$^{125}$I]apo-A-I), which exhibited immunological properties identical with those of apo-A-I, was a generous gift from C. Edelstein. Labeling was carried out by the lactoperoxidase procedure (Schonfeld, et al., 1977).

Water was deionized through a mixed-bed ion exchanger and then distilled in an all-glass apparatus. All buffers were freed from traces of surfactants by foaming at room temperature for 10 min. All chemicals were at least of reagent-grade purity.

### *Methods*

*Formation of Protein Monolayer at the Air–Water Interface.* The monolayer studies were conducted with either the surface area or the number of apo-A-I molecules kept constant (Evans et al., 1970). In the experiments in which the number of molecules was kept constant, an aliquot of an apo-A-I solution (0.1–0.2 mg/mL) containing ~10 μg of protein was spread (Trurnit, 1960) onto a subphase with a total area of 600 cm$^2$ from a Gilmont all-glass micrometer burette with its tip touching the side of a partially immersed glass rod at ~0.5 cm above the interface. The flow rate from the burette was 0.02 mL min$^{-1}$. Ten minutes after spreading, the film was compressed at a rate of 120 cm$^2$/min.

In the experiments at constant surface area, small aliquots of protein solution were successively spread, by the method described above, onto a subphase with a total area of either 70 or 127 cm$^2$. After each spreading, the surface pressure was monitored with a du Noüy ring connecting to the arm of a Cahn Electrobalance (Lagocki et al., 1973) until it reached a constant value. Repeated experiments showed that the experimental error in surface pressure was less than 0.1 dyn/mL. To determine the amount of protein at the interface, collected the monolayer at the completion of each experiment and quantified the amount of protein either by measuring the absorbancy at 206 nm or by counting the radioactivity of the iodine-125 labeled protein. The experimental error of this method was ~5%.

*Adsorption of Apo-A-I to the Air–Water Interface.* The amount of protein adsorbed from the solution onto an initially clean surface was measured by monitoring the changes in surface pressure. The concentration of the adsorbed monolayer was determined as follows. The monolayer, including some of the subphase solution, was swept into a graduate cylinder and its protein content was determined by absorbancy at 206 nm and fluorescamine assay. The surface concentration of the protein was obtained by dividing the excess amount of protein in this solution as compared to an equal volume of subphase solution for the total area of the air–water interface.

The kinetics of adsorption were studied with and without stirring of the subphase. Stirring was carried out with a glass-coated soft iron wire rotated at 60 rpm at a magnetic stirrer. At constant time intervals, the stirring was stopped for 10 s to permit accurate surface pressure determinations. A similar technique was used for measurements of the rate of desorption of spread protein monolayers.

The surface potential of the apo-A-I monolayers was measured by means of a copper electrode of 0.4 × 6 cm coated with 0.5 mCi of $^{210}$Po and a Beckman calomel reference electrode. The radioactive electrode was positioned 2–3 mm above the surface, and the potential was measured with a vibrating reed electrometer (Model 401, Cary).

The surface radioactivity of the [$^{125}$I]apo-A-I monolayer was monitored continuously by a radio chromatography system—Actograph III, Model 1002 (Nucleo Chicago)—equipped with an external detector (thin-layer conveyor system, Model 1006). The geiger counter, furnished with a Micromil window, was positioned 4 mm above the surface of the solution. The surface radioactivity detected was integrated every 10 s and plotted automatically on a Honeywell recorder.

*Determination of Diffusion Coefficient by Free Diffusion Method.* The apparent diffusion coefficient of apo-A-I was determined at 20 °C in an analytical ultracentrifuge with a Schlieren optics.[1] Initially, a sharp boundary was set up in a double-sector cell between a solution of apo-A-I (0.16 mg/mL) and a buffer solution. The concentration gradients $(\partial c/\partial x)_t$ and the distance ($x$) from the position of the initial boundary were then analyzed according to (Tanford, 1961)

$$\left(\frac{\partial c}{\partial x}\right)_t = -\frac{c_0}{2(\pi Dt)^{1/2}} e^{-x^2/(4DT)} \qquad (1)$$

where $c_0$ is the uniform protein concentration at $t = 0$ and $c$ is the concentration of protein along the axes of diffusion at any particular time $t$.

The apparent diffusion coefficient was then calculated from the slope of the straight line obtained by plotting $\ln |\partial c/\partial x|_t$ as a function of $x^2$.

## Results

The kinetics and the quantitation of spreading of apoprotein monolayers will be discussed first, followed by an analysis of the force–area curve of the monolayers and a parallel assessment of the surface concentration of the apoproteins by simple physical measurements.

*(A) Surface Properties of Apo-A-I. (1) Spreading of Apo-A-I.* The method described under Experimental Section yielded a quantitative spreading of apo-A-I, as indicated by the absence of any detectable protein in the subphase and by the quantitative recovery of protein in the monolayer. At pressures of less than 1 dyn/cm, the spreading of apo-A-I was a rapid process: the surface pressure increased instantly, and by the time the addition of the protein solution was completed, the surface pressure had reached a new constant value. As the surface concentration of the protein monolayer and hence the surface pressure increased, however, a slow, time-dependent increase in surface pressure was observed after each addition of protein solution. Initially, we attributed this phenomenon to the effect of surface shear viscosity of the protein monolayer (Rosano et al., 1975). However, the surface viscosity measurements on our material by Dr. de Feijter[2] using the concentric double-ring surface rheometer (de Feijter, 1979; de Feijter & Benjamin, 1979) ruled out this interpretation since

[1] B. W. Shen and F. J. Kézdy, unpublished results.

[2] J. de Feijter, unpublished observations.

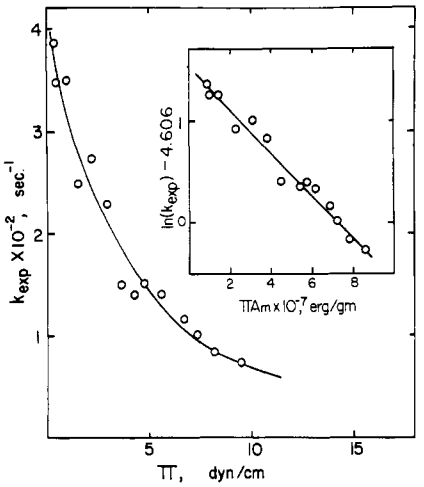


FIGURE 1: Surface-pressure dependence of the spreading constant for apo-A-I molecules at the air–water interface. Inset: analysis of data in the figure according to eq 6. Subphase: 0.01 M phosphate buffer, pH 7.6.

the viscosity of the apo-A-I monolayer was extremely low even at surface pressures as high as 10 dyn/cm. To understand the mechanism of the spreading phenomenon, we then turned our attention to the kinetics and pressure dependency of this process.

When small aliquots of protein were spread, the changes in surface pressure were found to be proportional to the changes in surface concentration within experimental error. With this linear approximation, we were able to study the kinetics of the spreading process, which we found to be first order with respect to the changes in surface pressure, i.e., $\Delta\Pi = \Pi_\infty - \Pi_t$ where $\Pi_\infty$ and $\Pi_t$ are the surface pressure at the end and at time $t$, respectively, of each spreading.

The first-order plot [i.e., ln ($\Delta\Pi$) vs. time] was linear over at least 80% of the time required for the process. The apparent first-order rate constant calculated from the slope of the straight line decreased with increasing surface pressure (Figure 1). By varying the amount as well as the volume of the protein spread, we observed that the first-order rate constant was a function of the surface pressure and was independent of both the protein concentration in the spreading solution and the amount of protein spread from each aliquot. These features ruled out diffusion of the protein into the surface as the rate-limiting step. They instead suggested that the rate-limiting step of the spreading process was the unfolding of the protein molecules which were already at the interface and that this process was proportional to the number of molecules in the "native" state, i.e.

$$dN/dt = k_u^0(N_\infty - N) = Qe^{-\Delta G^*/(RT)}(N_\infty - N) \quad (2)$$

where $N_\infty$ and $N$ are the number of unfolded molecules at time equal to $\infty$ and $t$, respectively. $Q$ is the probability factor for the molecule at its transition state to undergo forward reaction (i.e., unfolding). $\Delta G^*$ is the molar free energy of activation, and $k_u^0$ is the rate constant of unfolding at $\Pi = 0$. Since, as the pressure of the monolayer increased, each of the molecules newly arrived at the interface has to exert additional work ($\Pi A_m$) when colliding with the preexisting ones at the surface, eq 2 should be expressed on a molar basis as

$$dN/dt = k_{exp}(N_\infty - N) = Qe^{-(\Delta G^* + \bar{M}\Pi A_m)/(RT)}(N_\infty - N) \quad (3)$$

where $k_{exp}$ is the rate constant, $A_m$ (cm$^2$/g), and $\bar{M}$ (g/mol) are the average area and apparent molecular weight of the preexisting protein causing the newly spread molecule to decrease its rate of unfolding.

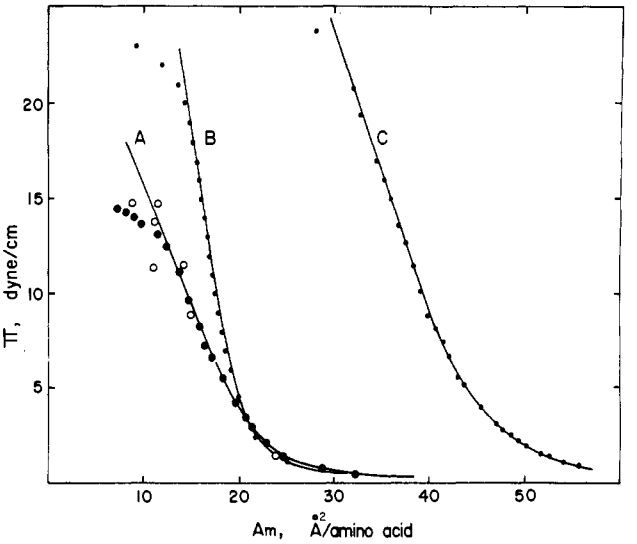


FIGURE 2: Force–area curve of apo-A-I monolayers. (A) Successive spreading; (B) fast compression, 10 min after spreading; (C) fast compression, 60 min after spreading. Open circles: results from adsorption. Subphase was as in Figure 1.

A comparison of eq 2 and 3 yields a relationship which predicts the pressure dependence of the spreading constant (eq 4):

$$k_{exp} = k_u^0 e^{-\bar{M}\Pi A_m/(RT)} \quad (4)$$

From the intercept and the slope of the linear ln $k_{exp}$ vs. $\Pi A_m$ plot (see inset, Figure 1), we can calculate $k_u^0 = 4.3 \times 10^{-2}$ s$^{-1}$ and $\bar{M} = 440$ g/mol. Assuming that monolayer mixing is a rapid process, the observed value of $\bar{M}$ is much smaller than the molecular weight of apo-A-I; this suggests that only a small portion of each preexisting molecule (in the order of a few amino acids) is involved in reducing the rate of unfolding of the newly spread molecules.

(2) *Apo-A-I Surface Isotherms.* The Π–A characteristics of monolayers of apo-A-I were dependent on the history of the monolayer (Evans, 1970). Three types of characteristic force–area isotherms were observed (see Figure 2). Curve A was obtained by successive spreading of small aliquots onto the constant surface area of a buffer solution. The results from six different preparations of apo-A-I were reproducible. The pressure shown in curve A is the final pressure of the apo-A-I monolayer after each spreading and thus corresponds to an equilibrium value. On the other hand, the compression of monolayers spread at low surface pressures did not always yield the same force–area curve. Rapid compression immediately after spreading yielded curve B, which deviates from curve A at pressures higher than 3 dyn/cm, presumably due to overcompression of the protein molecules. Slow aging of the monolayers at low pressure before compression shifted curve B upward until it reached curve C.

For a quantitative interpretation of the surface isotherms, the experimental data were divided into domains of low, intermediate, and high surface pressure. At low surface pressures (<0.5 dyn/cm), the force–area curves indicated that the protein monolayers obeyed the ideal gas equation proposed for dilute protein monolayers (Adamson, 1976)

$$\Pi(A - A_0) = nRT \quad (5)$$

where $A$ is the total surface area, $A_0$ is the limiting area occupied by $n$ mol of molecules, and $n$ is the number of moles at the interface. Equation 5 can be rewritten into the form

$$\Pi A/X = RT/M + (A_0/X)\Pi \quad (6)$$

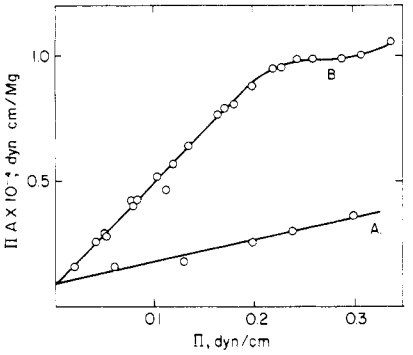


FIGURE 3: ΠA vs. Π plot of apo-A-I monolayer in the ideal gas region. (A) Data calculated from curve A, Figure 1; (B) data calculated from curve C, Figure 1.

Table I: Parameters of Surface Isotherm for Protein Monolayer at the Air-Water Interface

| protein | $A_{00}$ (Å²/ residue) | $k \times 10^2$ (cm/ dyn) | $B \times 10^{-6}$ erg/g | ref |
|---|---|---|---|---|
| apo-A-I A | 21.6 | 3.66 | 3.78 | this work |
| apo-A-I B | 20.6 | 1.32 | 4.27 | this work |
| apo-A-I C | 46.3 | 1.60 | 5.75 | this work |
| BSA | 15.6 | 1.64 | 1.14 | Evans et al. (1970) |
| β-casein | 19.2 | 3.17 | 2.95 | Evans et al. (1970) |
| hemoglobin | 15.5 | 1.74 | 1.14 | Pearson & Alexander (1968) |
| lysozyme | 16.4 | 1.98 | 0.94 | Pearson & Alexander (1968) |
| pepsin | 13.8 | 1.24 | 2.89 | Pearson & Alexander (1968) |
| trypsin | 5.6 | 2.77[a] | 0.79 | Pearson & Alexander (1968) |

[a] The value for trypsin was not considered in the discussion since no precaution was taken in the original study to prevent the autocleavage of trypsin.

where $X$ is the number of grams of protein spread at the surface and $M$ is the molecular weight of the protein species in the monolayer. As shown in Figure 3, all apo-A-I monolayers at low surface pressures obey eq 6; from the intercept on the ordinate axis, one obtains a molecular weight of (2.5 × 0.25) × $10^4$. The slope ($A_0/X$) increases progressively when the monolayer ages at low pressure. Compression immediately after spreading yielded a slope from which a limiting area of 24 Å²/amino acid was calculated. The slow aging of the monolayer ultimately yielded a value of $A_0$ as high as 66 Å²/amino acid.

In the intermediate pressure range (0.5–12 dyn/cm), the surface pressure increased curvilinearly with decreasing area. The data obtained for apo-A-I monolayer in this pressure range were found to best fit the empirical equation

$$A = A_{00} - A_{00}K\Pi + B/\Pi \quad (7)$$

The values of $A_{00}$, $K$, and $B$, listed in Table I, were obtainec by multiple regression fits of the data into eq 7. The values of $A_{00}$ and $K$ were found to be identical with the values of limiting area and compressibility modules extracted directly from the Π–$A$ curves. $B$ is a proportionality constant. Also listed in Table I are the surface parameters $A_{00}$, $K$, and $B$ obtained for a variety of globular protein isotherms (Evans et al., 1970; Pearson & Alexander, 1968) fitted with the help of eq 7. By using these parameters and eq 7, one can calculate the theoretical curve for the compression isotherms as shown in Figure 2, indicating that the difference between the theoretical curve and the experimental points is less than the experimental error. Deviations from the theoretical curve occurred only at very high surface pressures, where the protein monolayer presumably collapses.

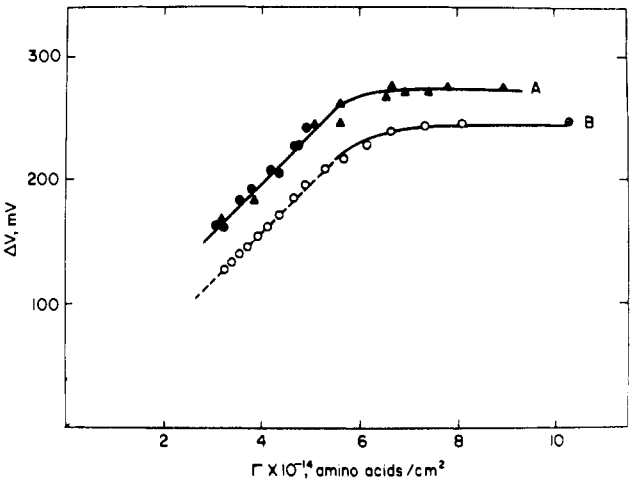


FIGURE 4: Surface potential vs. surface concentration plot of the apo-A-I monolayer. Curve A was obtained by successive spreading and curve B was obtained by fast compression. Subphase was as in Figure 1.

The data of Table I show that the limiting area for the apo-A-I molecule in the equilibrium spread monolayer is much smaller than that determined for the totally denatured molecule and yet significantly larger than the limiting area of globular proteins. Furthermore, the value of $A_{00}$ for apo-A-I (i.e., 22 Å²/amino acid) compares favorably with the value of 20 Å²/amino acid determined by Goupil & Goodrich (1977) for a monolayer of synthetic poly(γ-methyl-L-glutamic acid) in its pure α-helical conformations. Hence, we feel that the apo-A-I molecule at the interface maintains a substantial amount of two-dimensional secondary structure.

(*3*) *Surface Potential of Apo-A-I Monolayers.* The surface potential ($\Delta V$) of the apo-A-I monolayer formed either by rapid compression or by successive spreading increased linearly with increasing surface concentration up to ~5.5 × $10^{14}$ amino acids/cm² (18.2 Å²/amino acid) (see Figure 4). At higher surface concentrations, the surrface potential gradually became independent of the monolayer density. At all surface concentrations, the monolayer in spreading equilibrium (curve A, Figure 1) showed a potential ~30 mV higher than that of the rapidly compressed monolayer (curve B) at the same surface concentration. At surface concentrations less than 3 × $10^{14}$ amino acid/cm² (33 Å²/amino acid), the potential of the spread monolayer was not reproducible and decreased during aging of the monolayer at low pressure. The above observation is consistent with the view that, at low surface pressure, the apo-A-I molecules undergo a semiirreversible denaturation into random-coil conformation (curve C, Figure 1).

(*B*) *Kinetics of Surface Adsorption and Dissolution of Apo-A-I Molecules.* In agreement with reported observations (Camejo et al., 1968, 1970; Davis et al., 1973; Phillips et al., 1975a,b), the surface pressure of the apo-A-I solution increased rapidly with time, suggesting a time-dependent accumulation of surface-active material had occurred. The final pressure which was arrived at after repetitive compressions and expansions was dependent on the concentration of the protein solution and was found to be accompanied by a decrease in the concentration of the dissolved protein. The force–area and potential–area curves of the adsorbed apo-A-I monolayer coincided with those observed in the monolayer formed by successive spreading.

Since the time course for the surface accumulation of apo-A-I was orders of magnitude slower than that for the time

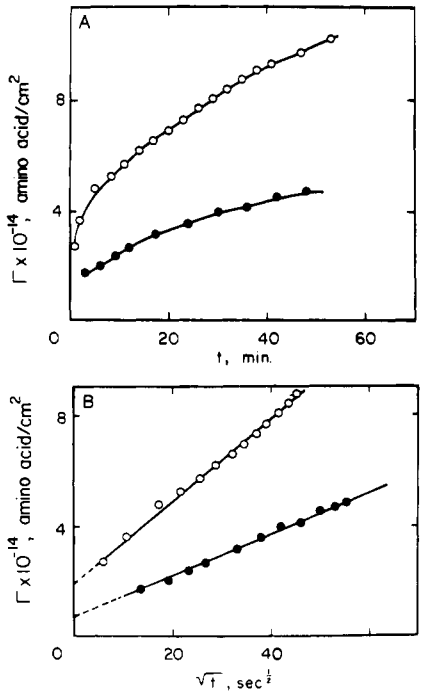


FIGURE 5: (A) Γ vs. $t$ isotherms for adsorption of apo-A-I to the air–water interface; nonstirred system; (B) Γ vs. $t^{1/2}$ plot for data in (A). Apo-A-I concentration in the solution is $1.19 \times 10^{16}$ (○) and $5.94 \times 10^{15}$ residues/cm³ (●). Buffer: 0.01 M phosphate, pH 7.6.

dependence of Π as described earlier by eq 3, when analyzing the adsorption kinetics, we therefore ignored the later process and assumed that the apo-A-I molecules reached the surface at spreading equilibrium. Thus, we analyzed the adsorption kinetics by converting surface pressure into surface concentration by using eq 7 and the parameters from curve A. The time course of the adsorption yielded a parabolic curve (Figure 5A), indicating that the surface adsorption is diffusion controlled (Ward & Tordai, 1946). The data were analyzed according to eq 8, which describes the rate law for diffusion-controlled adsorption:

$$\Gamma = 2C(D/3.1416)^{1/2}t^{1/2} + \text{constants} \qquad (8)$$

where Γ (amino acid/cm²) is the surface concentration of apo-A-I, $C$ (amino acid/cm³) is the protein concentration in the subphase, and $D$ (cm²/s) is the diffusion coefficient of apo-A-I. A plot of Γ versus $t^{1/2}$ gave a straight line (see Figure 5B). During the time course of our kinetic study, the protein concentration in the bulk phase, $C$, remained approximately constant; thus, the diffusion coefficient ($D$) could be calculated from the slope of the straight line in Figure 2B. The values of $D$ obtained at several protein concentrations were in good agreement with the apparent diffusion coefficient, $D_{w,20} = 1.25 \times 10^{-6}$ cm²/s, determined by the free diffusion method in the analytical ultracentrifuge.

If the formation of the stable apo-A-I monolayer is a diffusion-controlled process, the rate of monolayer formation should be increased markedly by continuous stirring of the subphase. The results for a stirring rate of 60 rpm showed that the adsorption of apo-A-I took plase initially at a constant rate which was at least 10 times faster than that for the unstirred system; the rate gradually leveled off and finally reached zero (Figure 6). Moreover, the steady rate of apo-A-I adsorption in the stirred system was linearly proportional to the protein concentration in the bulk phase (inset, Figure 6). Thus, initially the rate of monolayer formation was proportional to the rate of diffusion of apo-A-I molecules through

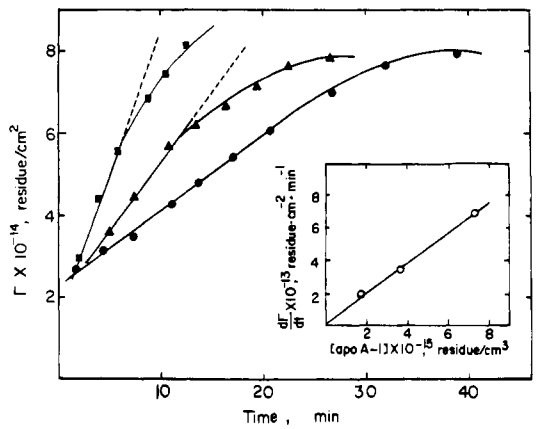


FIGURE 6: Adsorption of apo-A-I to the air–water interface by constant stirring of the subphase (stirring rate 60 rpm). Apo-A-I concentrations are $1.84 \times 10^{15}$ (●), $3.69 \times 10^{15}$ (▲), and $7.37 \times 10^{15}$ residues/cm³ (■).

Table II: Diffusion Coefficient of Apo-A-I Measured by Surface Adsorption

| $C \times 10^{-15}$ (amino acid/cm³) | pH | KCl (M) | $D_{w,20} \times 10^6$ (cm²/s) | stirring of the subphase |
|---|---|---|---|---|
| 2.92 | 7.8 | | 1.10 | – |
| 5.84 | 7.8 | | 1.30 | – |
| 11.63 | 7.8 | | 1.08 | – |
| 3.68 | 7.8 | | 1.13 | + |
| 3.68 | 7.4 | | 1.20 | + |
| 3.68 | 7.0 | | 1.19 | + |
| 3.68 | 6.6 | | 1.03 | + |
| 3.68 | 6.0 | | 1.35 | + |
| 1.83 | 7.8 | | 1.09 | + |
| 3.68 | 7.8 | | 1.13 | + |
| 7.35 | 7.8 | | 1.18 | + |
| 4.31 | 7.8 | 0.05 | 1.29 | + |
| 4.31 | 7.8 | 0.10 | 1.13 | + |
| 4.31 | 7.8 | 0.15 | 1.35 | + |
| 4.31 | 7.8 | 0.20 | 1.39 | + |

the unstirred delta layer, as predicted by the equation (Ter Minassian-Saraga, 1955)

$$d\Gamma/dt = (D/\delta)C \qquad (9)$$

where δ is the thickness of the unstirred δ layer. By using the diffusion coefficient calculated from the nonstirred system, we calculated the thickness of the δ layer to be $6 \times 10^{-2}$ cm for a stirring rate of 60 rpm. By using the same stirring rate, the adsorption of apo-A-I to the air–water interface was studied as a function of protein concentration, pH, and ionic strength; the results of these studies are shown in Table II. The finding that the $D$ values remained unchanged under various conditions indicates that the surface adsorption of apo-A-I molecules is a diffusion-controlled process.

To determine the relationship between the molecules at the interface and those in the solution, we measured the surface concentration of apo-A-I at the end of the adsorption, $\Gamma_e$, and plotted the values as a function of $C_e$, the final concentration of apo-A-I in the bulk phase. The results of these measurements, indicated that, at surface concentrations greater than $4 \times 10^{14}$ residues/cm², $\Gamma_e$ increased with increasing protein concentration and reached saturation at $\sim 1.5 \times 10^{15}$ rsidues/cm² (see Figure 7).

This observation suggested the existence of an equilibrium between the molecules at the surface and in the solution and thus a correlation between the rate of monolayer formation and the net adsorption of the molecules to the surface. We expected that as the adsorption progressed the fractional

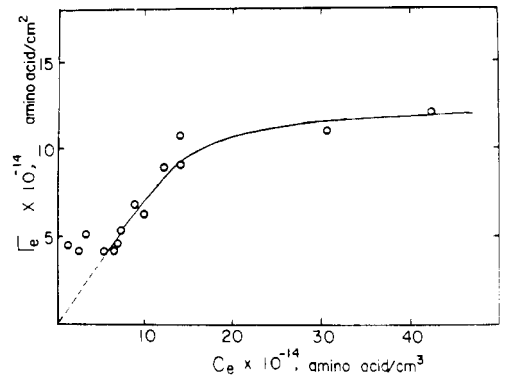


FIGURE 7: Equilibrium concentration of apo-A-I monolayer as a function of equilibrium protein concentration in the bulk phase.

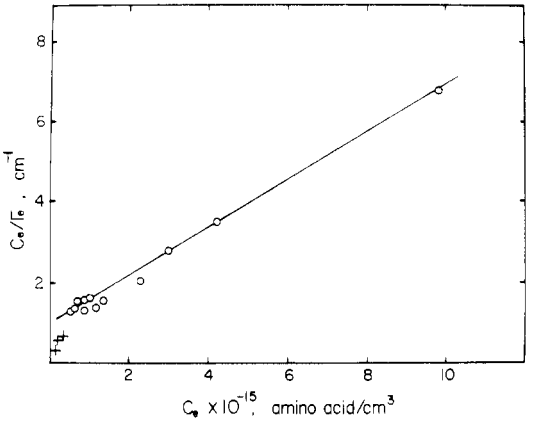


FIGURE 8: $C_e/\Gamma_e$ vs. $C_e$ plot of results shown in Figure 7. Results obtained at low concentrations (+) are not included in the analysis.

surface area already covered by molecules increased; in consequence, there was also an increase in the probability for a molecule reaching the interface to be desorbed. By assuming that the air–water interface had a definite number of adsorption "sites" with area $A_a$—which is the minimum area required for adsorption to occur—it was estimated that the fraction of the surface area free for further adsorption was $1 - A_a/A_m$ and that the formation of apo-A-I monolayer was governed by the following rate law (eq 10), which is smaller to the equation derived by Langmuir (1918) for the condensation and evaporation of gas onto a solid surface:

$$d\Gamma/dt = (D/\delta)C(1 - A_a/A_m) - k_s\Gamma \qquad (10)$$

where $k_s$ is the desorption rate constant.

Since at the beginning of the adsorption the interface is empty, eq 10 reduces to the form expressed in eq 9. At equilibrium, the net rate of adsorption becomes zero, and eq 10 can be rearranged into the following form with the substitution of $1/\Gamma_e$ for $A_e$, the molecular area of apo-A-I at equilibrium:

$$\frac{C_e}{\Gamma_e} = (\delta/D)k_s + A_aC_e \qquad (11)$$

When the values of $\Gamma_e$ and $C_e$ listed in Table III were analyzed according to this equation, all data points, except those obtained at low protein concentration, fitted a straight line perfectly with a correlation coefficient of 0.998 (see Figure 8). From the slope, the intercept on the ordinate, and the values of $D$ and $\delta$ determined earlier, we calculated that $k_s = 2.2 \times 10^{-4}$ s$^{-1}$ and $A_a = 6$ Å$^2$/residue. The good correlation between the experimental results and the theoretical equation argues for the existence of a rapid equilibrium between the molecules at the interface and in solution.

Table III: Surface and Bulk Concentrations of Apo-A-I at Equilibrium

| part[a] | $C_i$[d] $\times 10^{-15}$ (amino acid/cm³) | $\Pi_e$[e] (dyn/cm) | $\Gamma_e \times 10^{-14}$ (amino acid/cm²) | $C_e \times 10^{-14}$ (amino acid/cm³) |
|---|---|---|---|---|
| A[b] | 0.388 | 1.56 | 4.38 | 1.22 |
| | 0.52 | 1.25 | 4.1 | 2.49 |
| | 0.65 | 3.21 | 5.1 | 3.33 |
| | 0.78 | 1.3 | 4.11 | 5.29 |
| | 0.98 | 2.0 | 4.56 | 6.98 |
| | 1.37 | 6.8 | 6.15 | 9.91 |
| | 1.76 | 13.2 | 8.85 | 12.15 |
| | 1.96 | 13.4 | 9.03 | 14.09 |
| B[c] | 1.48 | 3.4 | 5.33 | 7.35 |
| | 1.84 | 8.65 | 6.8 | 8.84 |
| | 2.96 | 15.6 | 11.1 | 14.09 |
| | 4.61 | 15.5 | 10.91 | 30.61 |
| | 5.95 | 16.5 | 12.07 | 42.43 |
| | 11.87 | 18.2 | 14.96 | 98.13 |
| | | 19.7 | 15.90[f] | 162.0 |
| C | | 1.98 | 4.2 | 6.7 |

[a] Results in parts A and B were obtained from absorption experiments. Results in parts C were obtained by dissolution and by direct measurement of apo-A-I in solution by fluorescamine. [b] Total volume, 33 cm³; area, 20.4 cm². [c] Total volume, 50 cm³; area, 70.5 cm². [d] Initial protein concentration in the bulk phase. [e] Surface pressure at equilibrium. [f] Surface concentration of apo-A-I assessed by absorbancy at 206 nm.

Table IV: Dissolution Constant for Apo-A-I Monolayer Spread at the Air–Water Interface[a]

| $\Pi_i$ (dyn/cm) | $\Gamma_i \times 10^{-14}$ (amino acid/cm²) | $k_s \times 10^4$ (s$^{-1}$) |
|---|---|---|
| 10.9 | 4.14 | 2.0 |
| 10 | 4.02 | 2.3 |
| 8.8 | 3.8 | 2.6 |
| 5.1 | 3.15 | 2.1 |

[a] $\Pi_i$ and $\Gamma_i$ are the initial pressure and initial surface concentration, respectively.

The hypothesis that a fast equilibrium occurred between the molecules in the monolayer and in the subphase was also supported by the kinetics of monolayer desorption. In these experiments, the surface pressure of a spread monolayer decreased continuously upon constant stirring of the subphase. At the same time, the protein appeared in the subphase, indicating dissolution of the protein monolayer. The rate of dissolution ($-d\Gamma/dt$) was linearly proportional to the surface concentration of the protein monolayer with a slope equal to $k_s$, the rate constant of dissolution. The $k_s$ values listed in Table IV are in excellent agreement with the value derived from the slope of eq 9 and 10, showing that the distribution of the apoprotein molecules is diffusion controlled.

Further support for the existence of an equilibrium between the adsorbed molecules and those in solution was provided by studying the free exchange of radioactively labeled and cold apo-A-I. In these experiments, a solution of [$^{125}$I]apo-A-I (5 $\mu$g/mL, 1.25-mL total volume) was allowed to adsorb until reaching equilibrium. Then 1 mL of the subphase was slowly removed and replaced simultaneously by an equal volume of apo-A-I solution with identical protein concentration and the surface radioactivity was monitored by the method described in the experimental section. In addition to the abrupt change in radioactivity due to loss of [$^{125}$I]apo-A-I in the subphase, the surface radioactivity was found to decrease continuously over a period of several hours. This continuous loss of radioactivity was interpreted as the dissolution of [$^{125}$I]apo-A-I

from the interfacial region into the subphase, presumably through an exchange with the apo-A-I molecules arriving from solution. Furthermore, the time course for the free exchange was compatible with that of a nonstirred diffusion controlled process.

## Discussion

Our results show that at the air–water interface apo-A-I (1) spreads and unfolds readily from an aqueous solution, the rate and extent of unfolding being dependent upon the free area at the surface, (2) exists as a monomer, i.e., it does not form aggregates at the interface, and (3) exhibits two well-defined conformations—"native" and "denatured"—which differ from each other in their fundamental surface properties, particularly in the limiting area per amino acid ($A_{00}$) and in compressibility. The data also indicate that the denatured molecules are mainly in the random-coil structure, whereas the native molecules assume different structural conformations depending upon the surface pressure. All conformational isomers of the native molecules appear to be readily interconvertible and to have a distribution independent of the history of the protein molecule. Moreover, all conformational isomers of the native molecules seem to be in direct equilibrium with the apo-A-I molecule dissolved in the aqueous phase through a diffusion-controlled adsorption–desorption process.

The analysis of the surface properties of proteins can provide an insight into their general behavior at the air–water interface. In particular, the examination of the surface isotherms according to eq 7 shows that proteins with different physical properties can be classified according to their surface compressibility. A comparison of the $k$ values indicates that $\beta$-casein and apo-A-I have values in excess of $3 \times 10^{-2}$ cm/dyn, whereas the values for all of the other protein monolayers, including totally denatured apo-A-I, are below this level (Table I). In addition, apo-A-I and $\beta$-casein exhibit a high value of $A_{00}$ (above 20 Å$^2$/amino acid), whereas the value of $A_{00}$ for the well-organized globular proteins is well below 15 Å$^2$/amino acid. These results suggest that the surface activity of a protein molecule is closely related to its structural flexibility. However, $\beta$-casein, although highly surface active and flexible, lacks the conformational reversibility exhibited by the apo-A-I molecules. Therefore, the capacity of apo-A-I to fold and unfold readily at the interface is probably dictated by its primary sequence. A phylogenetic analysis (Fitch, 1977) has shown that a substantial part of the apo-A-I molecule contains repeating structural units of 11 residues, with hydrophobic and hydrophilic amino acids segregated on different sites of the helix when the amino acids are placed on an Edman helical wheel. Moreover, an analysis based on the free energy of stabilization and the Chou and Fasman potentials (Edelstein et al., 1979) showed that the entire apo-A-I molecule consists of amphiphilic helices connected by turns and coils which are also amphiphilic. Thus, it appears that the surface properties of apo-A-I are attributable to this internal structural organization. This concept is supported by the results obtained from studying the surface and lipid binding properties of synthetic peptides mimicking the sequence of apo-A-I (Kupferberg et al., 1979). Those authors showed that peptides with high $\alpha$ helicity and amphiphilicity exhibit surface properties similar to that of apo-A-I. Moreover, a 22-residue synthetic peptide with high $\alpha$-helical amphiphilicity was also shown to bind dimyristoylphosphatidylcholine (DMPC) liposomes and to stimulate lecithin cholesterol acyltransferase activity (Pownall et al., 1979).

The great ease by which apo-A-I in solution accumulated at the surface region suggests that this protein has a high structural adaptability to the environment, which has already been demonstrated in solution by Reynolds (1976), Tall et al. (1975), and Edelstein & Sakoda (1979). In light of this property, it is not surprising that the molecules at the surface are in thermodynamic equilibrium with those in solution. Figure 7 also indicates that equilibrium can occur only at surface concentrations higher than $5 \times 10^{14}$ amino acid/cm$^2$ (20 Å/amino acid) and that, upon dilution below this value, the protein denatures quasi-irreversibly, like other proteins at the air–water interface. Thus, the reversible adsorption–desorption of apo-A-I occurs only at a rather dense interface such as that provided by the lipoprotein and, in particular, HDL. This rapid equilibration between the apo-A-I molecules at the surface and those in solution may explain why some free apo-A-I's are found in solution during the preparation of HDL. We may surmise that, by analogy to the air–water interface, apo-A-I molecules in HDL are in equilibrium with the aqueous environment. Thus, information obtained at the air–water interface may shed some light on the spatial organization of apoproteins at the lipoprotein surface, although care must be exercised in directly extrapolating such data.

## Acknowledgments

The authors thank Dr. Ferenc J. Kézdy for his interest and support at the initial stage of this investigation, as well as for his helpful discussions and critical reading of the manuscript. We acknowledge the contribution of Drs. de Feijter and John H. Law for critical reading of this manuscript. We also thank Elisabeth F. Lanzl for professional editing and Janyce Nasgowitz for preparing the manuscript.

## References

Adamson, A. W. (1976) *Physical Chemistry of Surfaces*, 3rd ed., New York, N.Y., Chapter 2, pp 46–98, Wiley, New York.

Aggerbeck, L. P., Kézdy, F. J., & Scanu, A. M. (1976) *J. Biol. Chem. 251*, 3823–3830.

Baker, H. N., Dalahunty, T., Gotto, A. M., Jr., & Jackson, R. L. (1974) *Proc. Natl. Acad. Sci. U.S.A. 71*, 3631–3634.

Camejo, G. (1969) *Biochim. Biophys. Acta 175*, 290–300.

Camejo, G., Colacicco, G., & Rapport, M. M. (1968) *J. Lipid Res. 9*, 562–569.

Camejo, G., Suarez, A. M., & Munoz, V. (1970) *Biochim. Biophys. Acta 218*, 155–166.

Davis, M. A. F., Hauser, H., Leslie, R. B., & Phillips, M. C. (1973) *Biochim. Biophys. Acta 317*, 214–218.

de Feijter, J. (1979) *J. Colloid Interface Sci. 69*, 375–383.

de Feijter, J., & Benjamin, J. (1979) *J. Colloid Interface Sci. 70*, 375–382.

Edelstein, C., & Sakoda, N. (1979) presented at the 63rd Annual Meeting of the Federation of American Societies for Experimental Biology, Dallas, TX, April 1–10, 1979, p 308.

Edelstein, C., Kézdy, F. J., Scanu, A. M., & Shen, B. W. (1979) *J. Lipid Res. 20*, 143–153.

Evans, M. T. A., Mitchell, J., Mussell White, P. R., & Iron, L. (1970) in *Surface Chemistry of Biological Systems* (Blank, M., Ed.) pp 1–22, Plenum Press, New York.

Fitch, W. M. (1977) *Genetics 86*, 623–644.

Formisano, S., Brewer, H. B., & Osborne, J. C. (1978) *J. Biol. Chem. 253*, 354–360.

Goupil, D., & Goodrich, R. (1977) *J. Colloid Interface Sci. 62*, 142–148.

Kupferberg, J. P., Kroon, D. J., Yokoyama, S., Fukushima, D., Shen, B. W., & Kaiser, E. T. (1979) *Pept., Proc.* Sixth *Am. Pept. Symp., 6th* (in press).

Lagocki, J. W., Law, J. H., & Kézdy, F. J. (1973) *J. Biol. Chem. 248*, 580–587.
Langmuir, I. (1918) *J. Am. Chem. Soc. 40*, 1361–1403.
Morrisett, J. D., Jackson, R. L., & Gotto, A. M., Jr. (1975) *Annu. Rev. Biochem. 44*, 183–208.
Osborne, J. C., Jr., & Brewer, H. B., Jr. (1977) *Adv. Protein Chem. 31*, 253–337.
Pattnaik, N. M., Kézdy, F. J., & Scanu, A. M. (1976) *J. Biol. Chem. 251*, 1984–1989.
Pearson, J. T., & Alexander, A. E. (1968) *J. Colloid Interface Sci. 27*, 53–63.
Phillips, M. C., Evans, M. T. A., & Hauser, H. (1975a) *Adv. Chem. Ser. No. 144*, 217–230.
Phillips, M. C., Hauser, H., Leslie, R. B., & Oldani, D. (1975b) *Biochim. Biophys. Acta 406*, 402–414.
Pownall, H. J., Alben, J. J., Gotto, A. M., & Sparrow, J. T. (1979) presented at the 5th International Symposium on Atherosclerosis, Nov 6–9, 1979, Houston, TX, Abstract No. 109.
Reynolds, J. A. (1976) *J. Biol. Chem. 251*, 6013–6015.
Ritter, M. C., & Scanu, A. M. (1977) *J. Biol. Chem. 252*, 1209–1216.
Rosano, H. L., Chen, S. H., & Whittan, J. H. (1975) *Adv. Chem. Ser. No. 144*, 259–271.
Scanu, A. M., Toth, J., Edelstein, C., Koga, S., & Stiller, E. (1969) *Biochemistry 8*, 3309–3316.
Scanu, A. M., Lim, C. T., & Edelstein, C. (1972) *J. Biol. Chem. 247*, 5850–5855.
Schonfeld, G., Chen, J.-S., McDonneld, W. F., & Jeng, I. (1977) *J. Lipid Res. 18*, 645–655.
Shen, B. W., & Scanu, A. M. (1979) *ACS Symp. Ser. No. 81*, Abstract 57.
Shen, B. W., Scanu, A. M., & Kézdy, F. J. (1973) *Circulation, Suppl. 48 (IV)*, 218.
Silberberg, A. (1962) *J. Phys. Chem. 66*, 1872–1883.
Tall, A. R., Small, D. M., Shipley, G. G., & Lees, R. S. (1975) *Proc. Natl. Acad. Sci. U.S.A. 72*, 4940–4942.
Tanford, C. (1961) *Physical Chemistry of Macromolecules*, pp 353–356, Wiley, New York.
Ter Minassian-Saraga, L. (1955) *J. Chim. Phys. Phys.-Chim. Biol. 52*, 181–200.
Trurnit, H. J. (1960) *J. Colloid Sci. 15*, 1–13.
Vitello, L. B., & Scanu, A. M. (1976) *J. Biol. Chem. 251*, 1131–1136.
Ward, A. F. H., & Toradi, L. (1946) *J. Chem. Phys. 14*, 453–461.

# Lipid Bilayer Stability in Membranes. Regulation of Lipid Composition in *Acholeplasma laidlawii* As Governed by Molecular Shape†

Åke Wieslander,* Anders Christiansson, Leif Rilfors, and Göran Lindblom

ABSTRACT: The polar lipid composition in membranes of *Acholeplasma laidlawii* is extensively regulated as a response to environmental changes. In particular, the ratio between the dominating lipids monoglucosyldiglyceride and diglucosyldiglyceride is altered depending on temperature, configuration of incorporated fatty acids, and membrane cholesterol content. Synthesis of monoglucosyldiglyceride is stimulated by low temperature and saturated fatty acids but diminished by the presence of cholesterol. These factors are likely to affect the molecular geometry of the membrane lipids. Monoglucosyldiglyceride and diglucosyldiglyceride have wedge- and rodlike molecular shapes, respectively, that are modifiable to a certain extent. The packing constraints of lipids in amphiphilic aggregates, i.e., hydrocarbon–water interfacial area, hydrocarbon chain volume, and hydrocarbon chain length, are very important in determining the aggregate structure [Israelachvili, J. N., Mitchell, D. J., & Ninham, B. W. (1976) *J. Chem. Soc., Faraday Trans. 2 72*, 1525]. Pure monoglucosyldiglyceride forms a reversed hexagonal ($H_{II}$) phase structure with different fatty acid contents, while diglucosyldiglyceride forms a lamellar phase. However, the only lipid structure compatible with a functional biological membrane is the lamellar phase. Consequently, the balance between lipids forming lamellar and other mesophase structures must keep within certain limits. Here we show that the response in *A. laidlawii* lipid metabolism following external and internal stimuli can be predicted on the basis of molecular shapes and is necessary for the cell in order to maintain optimal membrane stability. Furthermore, the reduced capacity of *Acholeplasma* membranes to incorporate cholesterol is another consequence of this regulation, aiming at preservation of bilayer stability.

The functional state of biological membranes involves a dynamic cooperation between the physiologically active proteins and the lipid matrix. Most physicochemical investigations of these membranes have focused on the gel to liquid crystalline phase transition and its influence on lipid lateral packing (Engelman, 1971), growth temperature adaptation (McElhaney, 1974), permeability characteristics of water, ions, and other species (Razin, 1975a), enzyme and transport activities (Read & McElhaney, 1975; Silvius et al., 1978), and protein disposition (Verkleij, 1975).

Concerning the contribution of lipid polar head groups to membrane function and stability, little is known. However, the maintenance of a critical balance between lipids with different anionic polar head groups has been observed in *Escherichia coli* (Raetz, 1978). Recent findings also show that the activities of a very limited number of membrane-associated enzymes are dependent on a specific lipid surrounding (Sandermann, 1978).

Our previous investigations have focused on the relationships between physiological regulation mechanisms and physical

† From the Department of Microbiology, University of Lund, S-223 62 Lund, Sweden (Å.W., A.C., and L.R.), and the Division of Physical Chemistry 2, Chemical Centre, S-220 07 Lund, Sweden (G.L.). *Received February 14, 1980.* This work was supported by the Swedish Natural Science Research Council.

0006-2960/80/0419-3650$01.00/0 